NOTES *Bull. Chem. Soc. Jpn.,* ***66****, 3508—3510(1993)*

Determination of Trace Impurities in Corrosive Gases by Gas-Phase FTIR

Keiji Miyazaki* and Takako Kimura
Gases for Electronics, Air Liquide Laboratories, 5-9-9 Tokodai, Tsukuba, Ibaraki 300-26

(Received April 27, 1993)

Synopsis. Trace moisture and other potential impurities (CO_2, CH_4, C_2H_6, and alkyl halides) in HCl and in HBr gases were analyzed by gas-phase FTIR spectroscopic technique. The detection limit was estimated to be 100 ppb with 2 cm^{-1} spectral resolution for 5-min measurement time at 1.2 $kg\,cm^{-2}$ pressure, using an MCT detector and an 8-m-pathlength gas cell with BaF_2 windows.

Both hydrogen chloride (HCl) and hydrogen bromide (HBr) are frequently used as dry etchant gases in VLSI manufacturing processes. HBr is recognized particularly for its high selectivity, high anisotropicity without the presence of Freon-type gases, and high etching rate.1) Carbon-containing gases such as CF_4 are to be avoided because it reduces the selectivity in the etching stage.1) Also, moisture in these corrosive gases is not acceptable for corrosion reasons.2) Thus, both moisture-free and carbon-free etchant gases are required for semiconductor applications.

There are only a few hygrometric methods compatible with corrosive gases: dew point meter3) and Karl Fisher titration,4) but their detection limits are in the order of a few ppm. A gas chromatographic method is often used to analyze gaseous impurities, however its detection limit towards moisture is in the order of a few tens ppm. FTIR is, on the other hand, a sensitive and selective method to identify and quantify multiple IR-active impurities including H_2O. Several groups reported the H_2O analysis in HCl by gas-phase FTIR,5—7) but the matrix effect on absorbance was not well investigated, and calibrations with N_2 matrix was simply applied.

We had previously investigated capability and limitation of gas-phase FTIR for the trace moisture determination in HCl.8) Although a linear calibration curve was obtained with 30-ppb detection limit using an InSb detector and quartz windows, the slope was slightly smaller in HCl than in N_2, indicating the need for a calibration in the same matrix gas as the sample gas. In the present study, we have extended our investigation to the analysis of other impurities in HCl as well as the impurities in HBr by using an MCT detector and BaF_2 windows.

Experimental

General: The experimental setup is almost the same as what has been previously reported.8b) A mass flow controller is added to introduce standard gas mixtures other than the moisture into the matrix gas for calibration.

FTIR Spectrometer: An FTIR spectrometer (JIR-100, JEOL) is used to collect infrared spectra, utilizing a liquid-nitrogen-cooled MCT detector (narrow range), a Ge-on-KBr beamsplitter, and a glober light source.

Gas Cell: A long path gas cell (Mini-cell, Infrared Analysis) is equipped with gold-coated optics and BaF_2 windows, operated with 8-m pathlength.

Chemicals: Vapor phase of HCl (or HBr) is taken from a cylinder and purified with a dedicated purifier to remove moisture down to less than the detection limit. Standard gas mixtures of nitrogen-balanced 10 ppm CO_2, 10 ppm CH_4, 7.7 ppm Freon113 (1,1,2-trichloro-1,2,2-trifluoroethane), and 496 ppm HCl are diluted with the matrix gas for FTIR calibrations. Moisture (@22 ppm/N_2) is generated by a permeation device, and its concentration can be varied over 0.1—10 ppm in 50% or above HCl or HBr mixed with N_2.

Results and Discussion

Spectral Interference. HCl Matrix: Neither HCl or DCl has spectral interference with H_2O (3800 and 1600 cm^{-1}) or with CO_2 (2300 cm^{-1}). However, the main peaks of alkane-group hydrocarbons (3000 cm^{-1}) and CO (2200 cm^{-1}) completely overlap with those in HCl and DCl, respectively. Alkyl halides are found in HCl gas from their absorption in the region 1300—800 cm^{-1} with fairly easy assignment.

HBr Matrix: In contrast with HCl, interference-free regions for H_2O and CO_2 are extremely limited in HBr due to partial peak overlapping of DBr with H_2O, and that of HBr with CO_2. The highest peak of H_2O at 1653 cm^{-1} can be used for calibration while its peak at 3854 cm^{-1} is more difficult to detect due to rather high noise of the MCT detector in this region.

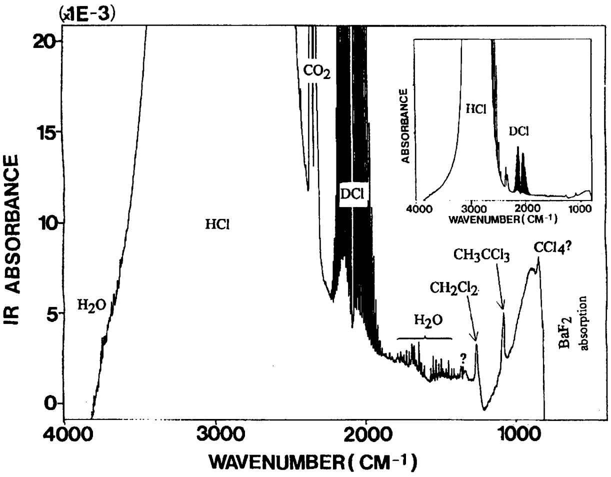

Fig. 1. Gas-phase infrared spectrum of HCl with H_2O, CO_2, DCl, and alkyl halides. Spectral resolution is 2 cm^{-1}.

Peaks of CO_2 (2360 cm^{-1}) is completely covered by HBr peaks while peaks of CO_2 at 3625 and 3720 cm^{-1} can be measured only with a 1—2 ppm detectability. Peaks of CO overlaps partially with the band edge of HBr, and sub-ppm measurement cannot be expected. Main peaks of alkane cannot be resolved due to the presence of a large amount of HCl in HBr. Detection of CH_4 and C_2H_6 in the 1300—1600 cm^{-1} region is possible if moisture is removed from the sample gas.

Consequently, impurities in HCl or HBr detectable in the region between 4000 and 800 cm^{-1} by FTIR are H_2O, CO_2, alkane-group hydrocarbons, and alkyl halides as shown in Figs. 1 and 2.

Spectral Shapes. H_2O Absorption Band: At 2 cm^{-1} spectral resolution, there was neither bandwidth broadening nor frequency shift in H_2O spectrum in either HCl or HBr matrix as compared with N_2. Absorption of H_2O peak at 1653 cm^{-1} was, however, reduced in height in both HCl and HBr matrices to the same extent, compared with that in N_2. At 0.25 cm^{-1} resolution, the bandwidth broadening and absorbance attenuation was clearly observed. The half-line width of H_2O absorption band at 1653 cm^{-1} in 50%HBr in N_2 was 0.75 cm^{-1}, similar to 0.79 cm^{-1} in 50%HCl in N_2 while it was 0.45 cm^{-1} in N_2 (Fig. 3). The H_2O absorption band at 3854 cm^{-1} in HCl and HBr matrices is also broadened compared with that in N_2. A collisional broadening effect on H_2O absorption (1653 cm^{-1}) was also confirmed in N_2 since varying the pressure between 1.0 and 2.0 kg cm^{-1} at 0.25 cm^{-1} resolution results in half-widths of 0.45 and 0.68 cm^{-1}, respectively.

Other Absorption Bands: Figures 4 and 5 show drastic changes of infrared absorption in the R-branch of HCl in HBr and 1306 cm^{-1} band of CH_4 in HBr: Both peak heights were increased in HBr compared with those in N_2. In particular, $H^{35}Cl$ peak at 2963 cm^{-1}

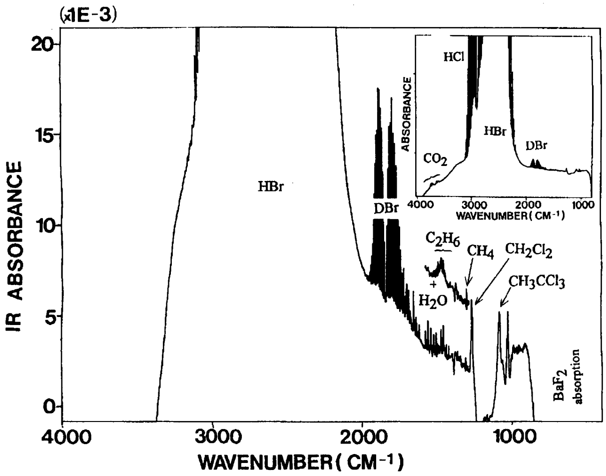

Fig. 2. Gas-phase infrared spectrum of HBr with HCl, H_2O, CO_2, DBr, alkane-group hydrocarbons, and alkyl halides. Peaks of CH_4 and C_2H_6 appear by passing through a purifier. Spectral resolution is 2 cm^{-1}.

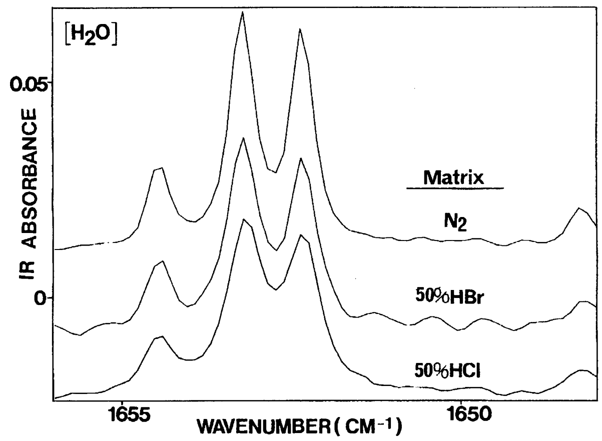

Fig. 3. Bandwidth broadening of H_2O peaks by 50% HCl/N_2 and 50% HBr/N_2 matrices in the 1653 cm^{-1} range. Spectral resolution is 0.25 cm^{-1}. H_2O concentration is 10 ppm.

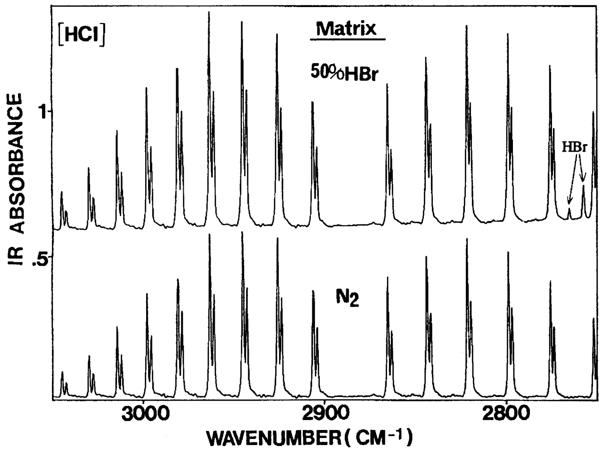

Fig. 4. Spectra of HCl in 50% HBr/N_2 and N_2 matrices. Spectral resolution is 1 cm^{-1}. HCl concentrations are ca. 670 and 500 ppm, respectively.

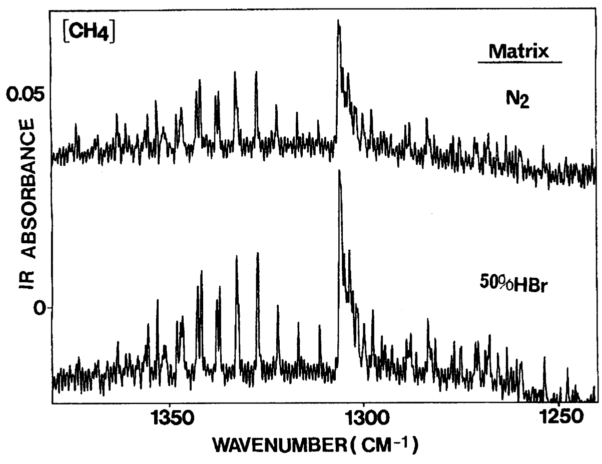

Fig. 5. Spectra of CH_4 in N_2 and 50% HBr matrices. Spectral resolution is 0.25 cm^{-1}. CH_4 concentration is 5 ppm.

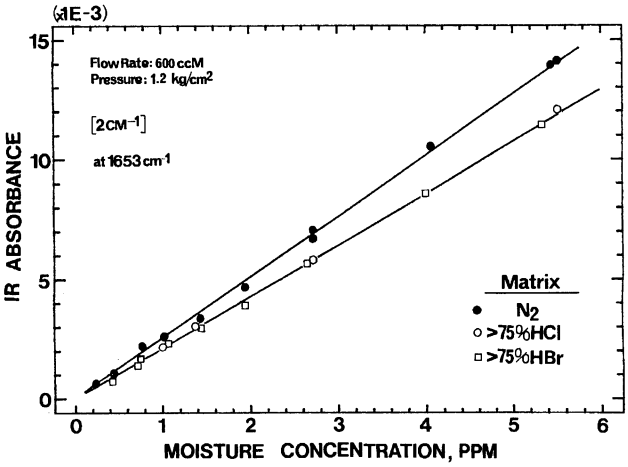

Fig. 6. Calibrations of H_2O in N_2, HCl, and HBr matrices at 1.2 kg cm^{-2} in 0.25—5.5 ppm range.

was extremely increased. Spectra of CO_2 in HCl and Freon113 in HBr were, on the other hand, identical to those in N_2.

These differences in spectral shapes between N_2 matrix and HCl/HBr matrix might be caused by difference in collisional broadening effect and/or perturbations in vibrational–rotational modes.[9—11]

Calibration of Potential Impurities. Infrared absorbance at 1653 cm^{-1} vs. concentration calibrations were carried out for 0.25—5.5 ppm of H_2O in N_2, in 95—75% HCl, and in 98—75% HBr at 1.2 kg cm^{-2} abs pressure, resulting in linear correlations in both matrices (Fig. 6). Their slopes in HCl and HBr matrices were reduced by 20% compared with that in N_2 matrix. The extent of absorption reduction was constant for >75% of HCl and HBr in N_2. Detection limits of H_2O in N_2, HCl, and HBr matrices, defined as a signal-to-noise ratio of 2, were estimated to be 100 ppb. A calibration curve of CO_2 (0.5—5 ppm) in 47—94% HCl in N_2 was linear and identical to that in N_2, whose detection limit was estimated to be 20 ppb. Single point calibrations of CH_4 (1306 cm^{-1} band) and Freon113 (816 cm^{-1} band) were carried out at 2 cm^{-1} resolution in 50% HBr/N_2 and in N_2. Detection limits of CH_4 and Freon113 were estimated to be 100 ppb and 20 ppb, respectively.

Gas-phasae FTIR technique is found to be very useful for trace and simultaneous determination of moisture and other carbon-containing impurities in corrosive gases (HCl and HBr) down to the sub-ppm level. This technique can be applied to qualify high purity (99.999%) HCl and HBr cylinder gases for semiconductor applications. Drastic changes of absorptions were, however, observed in the cases in H_2O in HCl/HBr, HCl in HBr, and CH_4 in HBr in comparison with those in N_2, requiring calibrations in the matrix gas which is the same as the sample gas.

References

1) M. Nakamura, K. Iizuka, and H. Yano, *Jpn. J. Appl. Phys.*, **28**, 2142 (1989).

2) D. K. Weber, S. J. Hardwick, W. O. Loos, and P. M. Bhadha, *Microcontamination*, **8**, 35 (1990).

3) E. Flaherty, C. Herold, and D. Murray, *Anal. Chem.*, **58**, 1903 (1986).

4) "Millipore's Microelectronics Application Note," August (1991).

5) D. E. Pivonka, *Appl. Spectrosc.*, **45**, 597 (1991).

6) W. I. Bailey, T. M. Booth, D. L. Grieble, and P. B. Henderson, "Proceedings on Technical Symposium for Semiconductor Process by Nihon Millipore," April (1992).

7) W. Plante, J. Jaillet, and R. Tawfik, "Microcontamination Conference Proceedings," p. 512 (1992).

8) a) K. Miyazaki, Y. Ogawara, and T. Kimura, "Abstracts of the 41st Annual Meeting in Jpn. Soc. Anal. Chem.," p. 74 (1992); b) K. Miyazaki, Y. Ogawara, and T. Kimura, *Bull. Chem. Soc. Jpn.*, **66**, 969 (1993).

9) C. L. Chaney and J. Chin, *Appl. Spectrosc.*, **28**, 139 (1974).

10) G. Herzberg, "Molecular Spectra and Molecular Structure II," Van Nostrand-Reinhold, New York (1945), p. 531.

11) G. Maes, A. Smolders, P. Vandevyvere, L. Vanderheyden, and T. Zeegers-Huyskens, *J. Mol. Struct.*, **173**, 349 (1988).